Automatic UAV Landing with Ground Target Maintained in the Field of View.

Laurent Burlion, H. De Plinval

Automatic UAV Landing with Ground Target Maintained in the Field of View

Laurent Burlion and Henry de Plinval

Abstract In this paper, a key feature for UAV visual servoing in automatic landing is investigated: the possibility to add an output constraint to a given control law, namely that a ground target point be maintained inside the camera field of view (FoV). This method has been recently developed, and the present study represents an application of this method, which can be applied to any nonlinear system. First, a control law for UAV automatic landing is proposed. Then, the output constraint method is presented. Later, the method is applied to the UAV landing case. Finally, simulation results confirm the effectiveness of the approach. The approach thus solves a key element of any visual servoing problem: the possibility to maintain a given object inside the camera field of view.

1 Introduction

Vision-based automatic UAV landing has been investigated in recent years. [26] proposed a linear visual servoing control scheme for the automatic hovering of a blimp. Later on, the same authors proposed in [27] a visual servoing scheme for vanishing features with application to UAV automatic landing. In [25], a nonlinear framework for UAV automatic landing is proposed based on 2D information from the camera image and the bi-normalised Plücker coordinates.
In these studies, a key assumption for practical implementation is that the object of interest is maintained inside the camera field of view along the landing trajectory. Some studies have considered implementing control laws so as to ensure this

Laurent Burlion
ONERA - The French Aerospace Lab, 2, avenue Edouard Belin, Toulouse, France, e-mail: laurent.burlion@onera.fr

Henry de Plinval
ONERA - The French Aerospace Lab, 2, avenue Edouard Belin, Toulouse, France, e-mail: henry.de-plinval@onera.fr

property. Thus, in [23], where this goal is reached through optimal paths computation and homography matrix switches. In [20], a rigid body is controlled while maintaining a target inside the field of view through Backstepping motion. In these works, smart strategies are proposed to avoid the object of interest getting out of the camera field of view. However, as far as automatic UAV landing is concerned, these strategies cannot be directly implemented, since they would lead to infeasible trajectories for such aircrafts: an aircraft cannot rotate at a given spot in space, and its linear / rotational velocities are not independent degrees of freedom.
In our approach, the so-called homography matrix is considered in order to maintain a given ground point inside the camera field of view. This matrix, which represents the image transformation corresponding to a change in the camera point of view, has been considered in various studies. In [15], this matrix is used to reconstruct the 3D structure based on two views. [16] uses a similar approach in the context of vision based car platooning. In [24], a complete visual map-less navigation is built upon the use of homographies. Studies have also investigated the analytical decomposition of the homography matrix in terms of position / orientation, as [17], a task which is fulfilled in [18]. Extensions have been proposed to the notion of homography, as the super-homography in [22]. In [19], a framework is proposed to control a robot based on information extracted from the homography matrix.
Output and Input hard constraints problems arise in most of the control applications and have been investigated in the past by many researchers. It is worth noting the input constraint problem is somewhat less difficult and has received more attention in the past few decades (see for instance [2]).
Existing solutions to both problems can be divided into two groups : those who check if the constraints will be violated by predicting the future and the other, which at each time, try to avoid the constraints. Concerning Linear systems, not only future prediction is easier but one can also apply some dedicated LMI-based methods [4, 13]. Moreover, state and input constraints problems are very close since there exists [7, 12] a relationship between a constrained output and an induced constrained input (whose constraints values are state dependent and so time-varying).
In a recent paper [1], we generalized this idea to nonlinear systems and it was shown how to transform one output constrained nonlinear system into one input constrained nonlinear system. By comparison to existing results [3, 8, 5, 9, 6, 10, 11, 14] (to cite a few), this method has several advantages : it does not use prediction and/or does not require the nonlinear system to be in any special form. However, this preliminary work only addressed the problem to constrain one output which is not sufficient to solve the applicative problem we propose to address in this paper.
This paper is organized as follows : the problem under consideration is presented in the first section. In Section 2, our main results are presented : after some theoretical developments, we show how one can transform the FoV constraints to some state-dependent saturation functions which are applied to the baseline flight control laws. In Section 3, we illustrate our results on our motivating example of a landing UAV and provide some numerical results. We finally give some conclusions and a future research direction.

1.1 Notations

Let $\mathscr{R}$ (resp. $\mathscr{N}$) denote the set of real numbers (resp. natural integers). In this paper, we are interested in nonlinear systems of dimension $n \in \mathscr{N}$. For $i \in [1,n]$, we note e_i the vector of the Euclidean basis of $\mathscr{R}^n$.

Given $\sigma \in \mathscr{C}^1(\mathscr{R}^n,\mathscr{R})$, $L_f\sigma := \sum_{i=1}^n f_i \partial_i \sigma$ denotes its Lie-derivative with respect to f.

Throughout this paper, we will use the following useful notations :

Given $r \in \mathscr{N}$ real numbers $K_1,\ldots,K_r$, we note

$$K_{j,r} := \prod_{i=j}^{r} K_i$$

and we also pose (for convenience) :

$$\forall j \in \mathscr{N},\ K_{j+1,j} := 1$$

Given two real numbers $z_{\min} < z_{\max}$, we note :

$$z \longmapsto Sat_{z_{\min}}^{z_{\max}}(z) = \max(z_{\min}, \min(z_{\max}, z))$$

the saturation function of a variable between $z_{\min}$ and $z_{\max}$

2 Problem statement

In this section, the problem under consideration is presented. The general problem under consideration is that of constraining a given function of the system's state in a desired range. In the present article, the case of an unmanned landing aircraft is addressed. We assume that this aircraft makes use of a videocamera for e.g. visual servoing purpose, for instance in order to improve its state estimate. This aircraft is controlled via a feedback aiming at maintaining it on a predefined landing trajectory. The goal of this paper is to show how, based on such a basic control law, the law can be modified so as to take into account an additional output constraint. In our case, this constraint consists in maintaining a given ground object inside the camera field of view.

2.1 Aircraft model

Throughout the paper, a linear assumption is made on the aircraft attitude -a landing aircraft showing typically low attitude angles. Note however that nonlinear elements do intervene in the model through the image model. The aircraft model is that of a classical aircraft, the main aerodynamics effects being taken into account. **To reduce the complexity of the computations carried in this paper, we directly control the aircraft by the angular velocity vector**

$$\omega := (p,q,r)^T$$

So, there is no need to compute the propulsion and aerodynamics momentums.
The acceleration of the aircraft is given by :

$$m\dot{V} = F_{aero} + F_{propu} \tag{1}$$

Moreover, the propulsion force is chosen such that the norm of the speed $\|V\|$ of the aircraft is constant during the landing phase ($\|V\| = V_0$).
Applying the hypothesis of small angles and some approximations, the **longitudinal dynamics** of the aircraft is the following one :

$$\begin{cases} \dot{z} & = V_0\gamma \\ mV_0\dot{\gamma} & = \frac{1}{2}\rho S V_0^2 C_{z\alpha}(\alpha - \alpha_{eq}^0) \\ \dot{\alpha} & = q - \dot{\gamma} \end{cases} \tag{2}$$

and the **lateral dynamics** of the aircraft is given by :

$$\begin{cases} \dot{x} & = V_0 \\ \dot{y} & = V_0\psi \\ \dot{\psi} & = \frac{g}{V_0}\varphi \\ \dot{\varphi} & = p \end{cases} \tag{3}$$

We assume that $\beta = 0$ and that $r = \frac{g\varphi}{V_0}$.
Coefficients are as follows:

$$\begin{cases} S & = 260m^2 \\ m & = 1,1.10^5 kg \\ C_{z\alpha} & = 5 \\ \alpha_{eq}^0 & = 3.7185deg \\ V_0 & = 70m.s^{-1} \\ g & = 9.81m.s^{-2} \\ \rho & = 1.225 \end{cases} \tag{4}$$

2.2 Image and homography

In the considered application case, a UAV makes use of a videocamera for e.g. state estimation improvement. As a result, it is required that given features on the ground be maintained inside the UAV field of view. This constraint is now computed as a function of the UAV state. To perform this computation, we make use of the so-called homography matrix, which is oftentimes used in visual servoing applications (see e.g. [15], [16], [24]). We shall suppose that a set of "reference" pictures of the landing runway have been taken along the desired landing trajectory. At every instant, one particular object described by a pointing direction in the reference image has to be maintained inside the videocamera field of view, a feature which can be used to maintain the runway inside the field of view, for instance. The homography matrix is computed from a comparison between the current and reference images (see e.g. [21, 19] for more details on homography matrices and associated computation algorithms). This matrix, which allows to transform the target's points coordinates from the reference pose to the current pose, is given by

$$H = R^T - \frac{1}{d^*} R^T p n^{*T} \tag{5}$$

where R, p, are the rotation matrix and translation vector from the current to the reference frame, d^* the distance from the UAV reference position to the target (ground) plane and n^* the normal to the target plane expressed in the reference frame. Now, based on this matrix, the current image coordinates of a ground object described by a pointing direction in the reference frame can be computed by computing first Hv^*, where v^* is this pointing direction. Then, the obtained vector $v = Hv^*$ is normalized (projection onto the image plane) through $w = (v_2/v_1; v_3/v_1)$. Now, this vector w is the 2D coordinates of the point in the current image. As a result, in order to maintain this point in the image field of view, one has to ensure:

$$-1 \leq w_1 \leq 1$$

and

$$-1 \leq w_2 \leq 1$$

Note that forcing rather for instance $-0.5 \leq w_2 \leq 0$ constraints the object to remain in a given sector of the current image. These constraint will be implemented in the considered application case.

For further computations, note that the derivative of the homography matrix is given by:

$$\dot{H} = -S(\omega)H - \frac{1}{d^*} \bar{v} n^{*T}$$

where $\bar{v}, \omega$ are the linear and angular velocities. Note that the image coordinate points could be computed directly, without computing the homography matrix; but this approach has been preferred in order to insist on its links to recent works on this topic.

2.3 Basic control design

The landing phase consists in following the trajectory :

$$x_c(t) = x(t) \; ; \; y_c(t) = 0 \; ; \; z_c(t) = x(t)tan(\gamma_c)$$

with $\gamma_c = -3deg$.
We note : $\delta_y = y - y_c, \delta_z = z - z_c, \delta_\alpha = \alpha - \alpha_{eq}^0$ and $\delta\gamma = \gamma - \gamma_c$.
Basic control laws are of the form :

$$\begin{cases} q = k_z\delta_z + k_\gamma\delta_\gamma + k_\alpha\delta_\alpha \\ p = k_y\delta_y + k_\chi\chi + k_\phi\phi \end{cases} \tag{6}$$

The coefficients are obtained by using classical Backstepping design and time scale separation hypothesis. (Of course, since the system to control is linear in this paper, other linear design like for instance LQ or poles placement can be used).
As an illustration (see figure (1)), we start the simulation with an initial error on z and y and we apply our control laws without taking into account our FoV constraints :

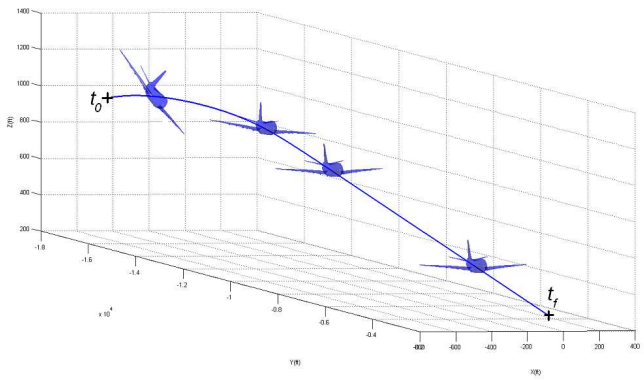

Fig. 1 Landing phase

2.4 Output constraint method

Our output constraint method (recently introduced in [1]) is based on a subtle transformation of the output constraint into an input saturation. Let us recall here the main principles of the method when one has one single output z to restrict inside a given interval $[z_{\min}, z_{\max}]$ when the system is controlled by a single input u.
So, let us consider the following class of nonlinear systems

$$\begin{cases} \dot{x} = f(x) + g(x)u \\ z = \sigma_1(x) + \sigma_2(x)u \end{cases} \tag{7}$$

where the functions f, g, σ_1, σ_2 are $\mathscr{C}^\infty$, $x \in \mathscr{R}^n$ is fully measured, the control u and the constrained output z belong to $\mathscr{R}$.
Let us now analyze the problem and give the main ideas which lead to our method :

1. it is necessary to compute the relative degree 'r' of the constraint output with respect to the input which is the number of times one has to derivate the output to make the input appeared in its 'r'th order derivative. Let us note this quantity: $r = d_u^{rel} z$.
2. one can then make the following remarks :
   - when $d_u^{rel} z = 0$ (i.e when $\sigma_2 \neq 0$) the output depends on the input and there is a strict equivalence between limiting the input u and the output z :

     $$z \in [z_{\min}, z_{\max}] \Leftrightarrow u \in \left[\frac{z_{\min} - \sigma_1}{\sigma_2}, \frac{z_{\max} - \sigma_1}{\sigma_2} \right]$$

   - when $d_u^{rel} z = 1$, we have :

     $$\dot{z} = L_f \sigma_1 + L_g u \quad \textit{where } L_g \neq 0$$

     In this case, the temptation is to propose a 'switching' control law u which verifies :

     $$\begin{cases} L_g u \leq -L_f \sigma_1 & \textit{when } z = z_{\max} \\ L_g u \geq -L_f \sigma_1 & \textit{when } z = z_{\min} \end{cases}$$

     However, this law has several drawbacks :
     – it leads to a 'switching law' and no more to a saturation on u
     – it does not seem possible to extend its design to a relative degree $d_u^{rel} z$ strictly superior to 1.
3. going back to the relative degree 1 case and given any constant $K > 0$, if one applies the following constraint :

   $$\dot{z} \in [-K(z - z_{\min}), -K(z - z_{\max})] \tag{8}$$

   z will remain inside $[z_{\min}, z_{\max}]$ provided its nominal value is inside this interval. Let us note that this is equivalent to apply the following input saturation :

   $$L_g u \in [-L_f \sigma_1 - K(z - z_{\min}), -L_f \sigma_1 - K(z - z_{\max})] \tag{9}$$

   we thus obtain an input constraint and what is interesting in this new problem position is the fact this constraint transformation can be iteratively applied when $d_u^{rel} z > 1$.
   Indeed, for instance if $d_u^{rel} z = 2$, one will apply two times a condition of the form (9). First, given $K_1 > 0$, one would like to apply

$$\dot{z} \in [-K_1(z - z_{\min}), -K_1(z - z_{\max})] \tag{10}$$

However, it is not possible to apply directly this constraint to our system since $d_u^{rel} z = 2$ (and thus $\dot{z}$ does not contain u). So, we note

$$\begin{cases} \dot{z}_{\min} := -K_1(z - z_{\min}) \\ \dot{z}_{\max} := -K_1(z - z_{\max}) \end{cases}$$

given $K_2 > 0$, it is required that

$$\ddot{z} \in [-K_2(\dot{z} - \dot{z}_{\min}), -K_2(\dot{z} - \dot{z}_{\max})] \tag{11}$$

This time this constraint is equivalent to a constraint on the control u since $d_u^{rel} z = 2$. At the end, our method amounts keeping the trajectory $t \longmapsto (z(t), \dot{z}(t), \ddot{z}(t))$ between two hyperplanes of the space $(z, \dot{z}, \ddot{z})$ (as illustrated below).

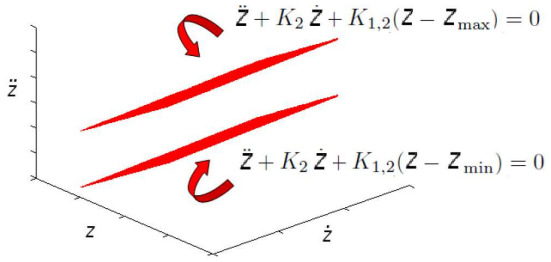

Fig. 2 Relative degree 2 case

In order to apply this method to the landing problem in presence of a FoV constraint, we here give an extension of the first theorem of ([1]). This extension consists in extending the result to several outputs and inputs.

Theorem 1 Let us consider the class of nonlinear systems (7) for which the full state is measured (i.e $y = x$) and z and u both belong to $\mathscr{R}^2$. Let us consider four real numbers which verify $z^1_{\min} < z^1_{\max}$ and $z^2_{\min} < z^2_{\max}$. We note $z = [z_1, z_2]^T$, $u = [u_1, u_2]^T$, $g = [g_1\ g_2]$ and $\sigma(x) = [\sigma_1(x), \sigma_2(x)]$.
Suppose z_1 (resp. z_2) is of relative degree $r_1 \in \mathscr{N}_{>0}$ (resp. r_2) and that the following 2×2 matrix $M_z(x)$ is invertible for all $x \in \mathscr{R}^n$

$$M_z(x) := \begin{matrix} L_{g_1} L_f^{r_1 - 1} \sigma_1(x) & L_{g_2} L_f^{r_1 - 1} \sigma_1(x) \\ L_{g_1} L_f^{r_2 - 1} \sigma_2(x) & L_{g_2} L_f^{r_2 - 1} \sigma_2(x) \end{matrix}$$

Suppose also that there exist $K^1_1, \ldots, K^1_{r_1} > 0$ and $K^2_1, \ldots, K^2_{r_2} > 0$ such that the initial state $x(0)$ satisfies the following conditions :
$\forall k \in [1,2], \forall j \in [0, r_k - 1]$,

$$K^k_{1,j} z_{k,\min} \leq \sum_{i=0}^{j} K^k_{i+1,j} L^i_f \sigma_k(x(0)) \leq K^k_{1,j} z_{k,\max}$$

then it is possible to find a state-dependent saturation for the control law u such that z_1 (resp.z_2) will remain in the set $[z_{1,\min}, z_{1,\max}]$ (resp.$[z_{2,\min}, z_{2,\max}]$).

Proof: By definition of the relative degrees r_1 and r_2, we have :

$$\begin{matrix} z_1^{(r_1)} \\ z_2^{(r_2)} \end{matrix} = \begin{matrix} L_f^{r_1}\sigma_1(x) \\ L_f^{r_2}\sigma_2(x) \end{matrix} + M_z(x) \begin{matrix} u_1 \\ u_2 \end{matrix}$$

If we pose :

$$\begin{matrix} \Gamma_1 \\ \Gamma_2 \end{matrix} := M_z(x) \begin{matrix} u_1 \\ u_2 \end{matrix}$$

the constrained outputs are decoupled with respect to the inputs Γ_1, Γ_2 i.e Γ_1 (resp. Γ_2) will be used to keep z_1 (resp.z_2) inside its interval.
For $k \in [1,2]$, applying the Theorem 1 of [1], we know that if the input Γ_k is kept inside $[h^k_1(x), h^k_2(x)]$ where :

$$\begin{matrix} h^k_1(x) = K^k_{1,r_k} z^k_{\min} - \sum_{i=0}^{r_k} K^k_{i+1,r_k} L^i_f \sigma_k(x) \\ h^k_2(x) = K^k_{1,r_k} z^k_{\max} - \sum_{i=0}^{r_k} K^k_{i+1,r_k} L^i_f \sigma_k(x) \end{matrix}$$

the output z_k will remain inside $[z_{k,\min}, z_{k,\max}]$ provided the initial state satisfies $\forall j \in [0, r_k - 1]$:

$$K^k_{1,j} z_{k,\min} \leq \sum_{i=0}^{j} K^k_{i+1,j} L^i_f \sigma_k(x(0)) \leq K^k_{1,j} z_{k,\max}$$

The proof is completed by going back to the inputs u_1 and u_2. We note u_1^{sat} and u_2^{sat} the corresponding saturated outputs. Indeed, since M_z is invertible, saturating Γ_k by $Sat^{h^k_2(x)}_{h^k_1(x)}$ leads to :

$$\begin{aligned} \begin{matrix} u_1^{sat} \\ u_2^{sat} \end{matrix} &= [M_z(x)]^{-1} \begin{matrix} Sat^{h^1_2(x)}_{h^1_1(x)}(\Gamma_1(x)) \\ Sat^{h^2_2(x)}_{h^2_1(x)}(\Gamma_2(x)) \end{matrix} \\ &= [M_z(x)]^{-1} \begin{matrix} Sat^{h^1_2(x)}_{h^1_1(x)} \left(e_1^T M_z(x) \begin{matrix} u_1 \\ u_2 \end{matrix} \right) \\ Sat^{h^2_2(x)}_{h^2_1(x)} \left(e_2^T M_z(x) \begin{matrix} u_1 \\ u_2 \end{matrix} \right) \end{matrix} \end{aligned}$$

2.5 Output constraint application to a landing aircraft

Along the aircraft landing trajectory, as earlier explained, a series of reference images are taken from the reference trajectory. For a given reference image i, corre-

sponding to the point of the reference trajectory at time t_i, at every time instant is associated the "error position" $\bar{\delta}_x = x(t) - x_c(t_i), \bar{\delta}_y = y(t) - y_c(t_i), \bar{\delta}_z = z(t) - z_c(t_i)$. With these variables and the aforementioned expression of the homography matrix, given the direction $[v_1^*; v_2^*; v_3^*]$ of the ground point in the reference image, one can compute the linearized homography matrix and the coordinates of the ground point in the current image frame according to:

$$\begin{cases} v_1 := v_1^* + v_2^*\psi - v_3^*\theta \\ v_2 := v_1^*\left(-\psi + \frac{\bar{\delta}_y \tan(\gamma_c)}{|z_c(t_i)|}\right) + v_2^* + v_3^*\left(\phi - \frac{\bar{\delta}_y}{|z_c(t_i)|}\right) \\ v_3 := v_1^*\left(\theta + \frac{\bar{\delta}_z \tan(\gamma_c)}{|z_c(t_i)|}\right) - v_2^*\phi + v_3^*\left(1 - \frac{\bar{\delta}_z}{|z_c(t_i)|}\right) \end{cases}$$

We verify that $\forall t,\ v_1 \neq 0$.
The outputs, which are the normalized image coordinates of the considered ground point, as presented earlier, are given by:

$$w_1 := \frac{v_2}{v_1} \qquad \& \qquad w_2 := \frac{v_3}{v_1}$$

we want to keep them inside $[-1, 1]$, for the point to be maintained inside the camera field of view. Moreover, the inputs are p and q, so the relative degrees of the outputs with respect to the inputs are $r_1 = r_2 = 1$.
In order to apply our main theorem, a few computations show that it is necessary for the following matrix to be invertible :

$$M_z(x) = \frac{1}{v_1} \begin{matrix} v_3^* & v_3^* w_1 \\ -v_2^* & v_1^* + v_3^* w_2 \end{matrix}$$

Since $v_1 \neq 0$ and $v_3^* \neq 0$, M_z is invertible iff :

$$v_1^* + v_2^* w_1 + v_3^* w_2 \neq 0$$

in other words, the outputs can be maintained inside their constraints iff they respect their constraints at $t = 0$ and the following geometrical condition is satisfied:

$$\mathbf{v}^{*T} \begin{matrix} 1 \\ w_1 \\ w_2 \end{matrix} \neq 0 \tag{12}$$

Now, this condition has a simple geometrical interpretation: it is the scalar product of the vector v^* -the direction of the target point in the reference image- with the vector $[1, w_1, w_2]^T$ -the direction of the target point in the current image. Thus, the condition is that these vectors be not perpendicular to each other. Indeed, if these vectors are perpendicular, then the image coordinates of the point is no more controllable from the two controls at hand: moving in one or the other direction does not change one of the point image coordinates, thus rendering the constraint impossible to satisfy. Now, this condition cannot happen if the ground point vector v^* is

not chosen on the edge of the image, and with the constraint being satisfied at the initial time and later on from the output constraint method. Indeed, with a 45 ° field of view camera, the two vectors cannot be perpendicular since they are both inside the camera field of view.

In order to apply our theorem, we compute f_w such that $\dot{w}_1$ and $\dot{w}_2$ are of the form :

$$\begin{matrix}\dot{w}_1 \\ \dot{w}_2\end{matrix} = f_w(x) + M_z(x) \begin{matrix}p \\ q\end{matrix}$$

Since $r_1 = r_2 = 1$ and the constrained variables are kept inside $[-1,1]$, we deduce the following limits of our inputs saturations for $k \in [1,2]$

$$\begin{aligned} h_1^k(x) &= -K_1^k(w_k+1) - e_k^T f_w(x) \\ h_2^k(x) &= -K_1^k(w_k-1) - e_k^T f_w(x) \end{aligned}$$

Taking the baseline control law $[p,q]$, we finally apply to the system the following control law $[p^{sat}, q^{sat}]$:

$$\begin{matrix}p^{sat} \\ q^{sat}\end{matrix} = [M_z(x)]^{-1} \begin{matrix}Sat_{h_1^1(x)}^{h_2^1(x)}\left(\frac{v_3^* p + v_3^* w_1 q}{v_1}\right) \\ Sat_{h_1^2(x)}^{h_2^2(x)}\left(\frac{-v_2^* p + (v_1^* + v_3^* w_2) q}{v_1}\right)\end{matrix}$$

3 Simulation results

In this section, we present the simulation results with the above presented aircraft model and control scheme. Figures 3 and 4 shows the UAV trajectory seen from a longitudinal viewpoint. The effect of the output constraint can be seen on the green lines: it introduces slight modifications in the trajectory, intended at maintaining the ground object inside the field of view.

Similarly, Fig.5 shows the trajectory seen from a lateral viewpoint. One more time, the outputs constraints introduce slight modifications on the trajectory.

The evolution of the constraint variables (e.g. w_1, w_2) is presented on Fig. 7. On this figure, the discontinuities correspond to the jumps between one reference image and the next one, as represented on Fig. 6. Indeed, each time a jump in reference image occurs, a new ground point is chosen, wrt to this new reference image; this new runway point is further on the runway, so that the constraint variable is reduced. As the aircraft keeps flying, the variable slowly increases, for the ground point moves toward the edge of the current image. Without the output constraint method, the output constraint variable increases beyond its allowed limit, while the output constraint method manages to maintain it inside its allowed variation range.

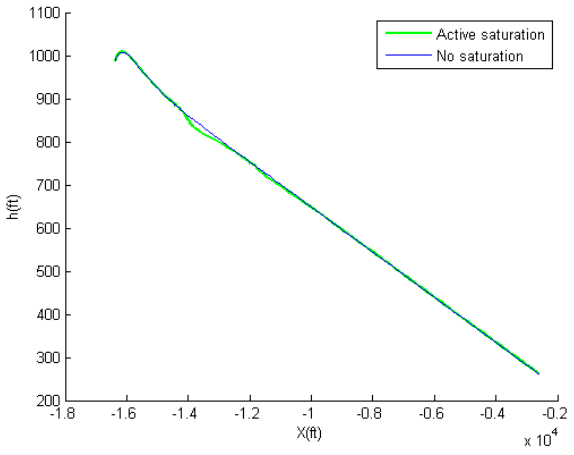

Fig. 3 Longitudinal trajectory view

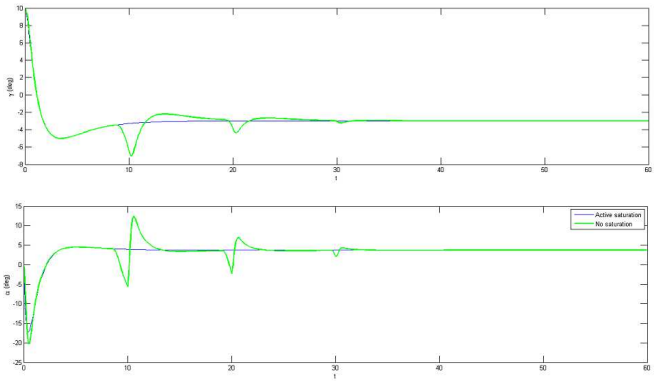

Fig. 4 Longitudinal trajectory angles

Finally, Fig. 8 shows the evolution of the control variables; the green lines represent the output constrained case; it can be seen that the method has a visible effect on the control variables, which in turns ensure the constraint to be fulfilled.

4 Conclusion

In this paper, a control law able to have a UAV automatically landing while maintaing a ground target point inside a videocamera field of view has been proposed. To this end, a recently developped output constraint method was used, and its application to this case was presented. One must notice the importance of this result:

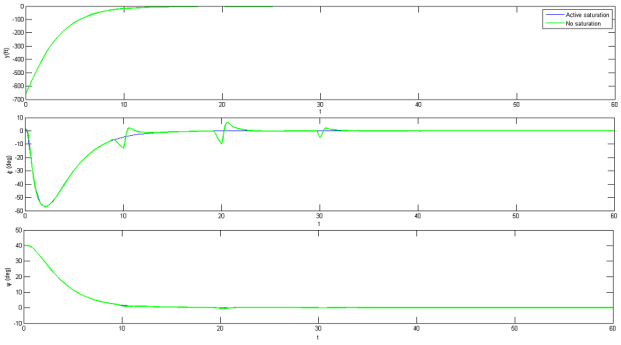

Fig. 5 Lateral trajectory view

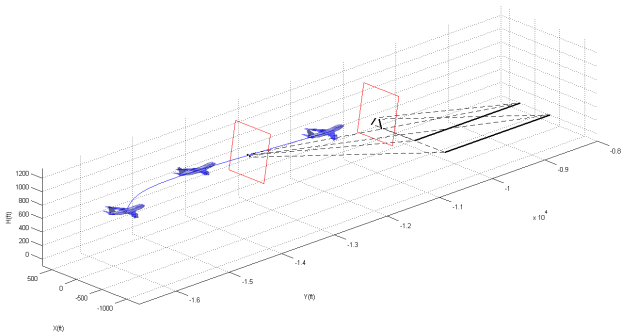

Fig. 6 Sequence of images

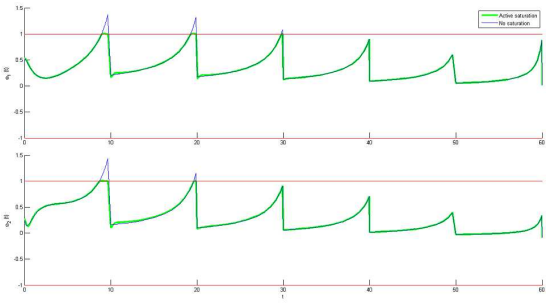

Fig. 7 $w_1(t)$, $w_2(t)$ and their constraints

indeed, most visual servoing studies make the assumption that the target does not exit outside the camera field of view, while this requirement is forced in our control scheme. This method thus opens new prospectives in the visual servoing field.

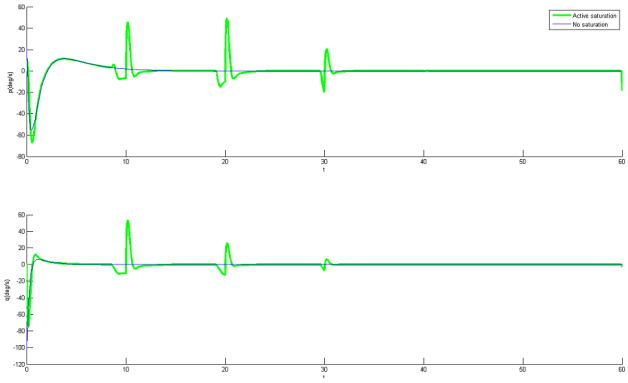

Fig. 8 Evolution of the control variables

References

1. L. Burlion, *A new Saturation function to convert an output constraint into an input constraint*, 20th Mediterranean Conference on Control and Automation, pp. 1217-1222, 2012.
2. D.S. Bernstein and A. N. Michel, *A chronological bibliography on saturating actuators*, International Journal of Robust and Nonlinear Control, vol.5, pp. 375-380, 1995.
3. F. Allgöwer and A.Z. Zheng, *Nonlinear model predictive control : assessment and future directions for research*, Progress in Systems and control Series, Birkhäuser Verlag, Basel, 2000.
4. T. Hu, *Nonlinear feedback laws for practical stabilization of systems with input and state constraints*, Proc. of the 47th Conference on Decision and Control, Cancun, Mexico, pp. 3481-3486, 2008.
5. P. Mhaskar, N.H. El-Farra and P.D. Christofides, *Stabilization of nonlinear systems with state and control constraints using Lyapunov-based predictive control*, Syst. & Contr. Lett., vol. 55, pp. 650-659, 2006.
6. K.B. Ngo, R. Mahony and J. Zhong-Ping, *Integrator backstepping using barrier functions for systems with multiple state constraints*, Proc. of the 44th Conference on Decision and Control, Seville, Spain, pp. 8306-8312, 2005.
7. E.G. Gilbert and K.T. Tan, *Linear systems with state and control constraints: the theory and application of maximal output admissible sets*, IEEE Transactions on Automatic Control, vol.36(9), pp. 1008-1020, 1991.
8. E. Gilbert and I. Kolmanovsky, *Nonlinear tracking control in the presence of state and control constraints : a generalized reference governor*, Automatica, vol.38, pp. 2063-2073, 2002.
9. K. Graichen and M. Zeitz, *Feedforward control design for finite-time transition problems of nonlinear systems with input and output constraints*, IEEE Transactions on Automatic Control, vol.53(5), pp. 1273-1278, 2008.
10. K.P. Tee, S.S. Ge and E.H. Tay, *Barrier Lyapunov functions for the control of output-constrained nonlinear systems*, Automatica, vol.45(4), pp. 918-927, 2009.
11. J.R. Cloutier and J.C. Cockburn, *The state-dependent nonlinear regulator with state constraints*, Proc. of the American Control Conference, Arlington, Texas, pp. 390-395, 2001.
12. O.J. Rojas and G.C. Goodwin, *A simple anti-windup strategy for state constrained linear control*, Proc. of the 15th IFAC World Congress, Barcelona, Spain, 2002.
13. M.C. Turner and I. Postlethwaite, *Output violation compensation for systems with output constraints*, IEEE Transactions on Automatic Control, vol.47(9), pp. 1540-1546, 2002.

14. M. Bürger and M. Guay, *Robust Constraint Satisfaction for Continuous-time Nonlinear Systems in Strict Feedback Form*, IEEE Transactions on Automatic Control, vol.55(11), pp. 2597-2601, 2010.
15. Z. Zhang and A. R. Hanson, *3D Reconstruction Based on Homography Mapping*, In ARPA Image Understanding Workshop, pp. 0249-6399, 1996
16. S. Benhimane and E. Malis and P. Rives J. R. Azinheira, *Vision-based Control for Car Platooning using Homography Decomposition*, IEEE Conference on Robotics and Automation, pp. 2161-2166, 2005
17. M. Vargas and E. Malis, *Visual servoing based on an analytical homography decomposition*, IEEE Conference on Decision and Control and European Control Conference, pp. 5379-5384 , 2005
18. E. Malis and M. Vargas , *Deeper understanding of the homography decomposition for vision-based control*, INRIA technical report, 2007
19. S. Benhimane and E. Malis , *Homography-based 2D Visual Tracking and Servoing*, International Journal of Robotic Research, pp. 661-676, 2007
20. R. Cunha and C. Silvestre and J.P. Hespanha and A. P. Aguiar, *Vision-based control for rigid body stabilization*, Automatica, pp. 1020-1027, 2011
21. E. Malis and P. Rives , *Robustness of Image-Based Visual Servoing with Respect to Depth Distribution Errors*, IEEE International Conference on Robotics and Automation, pp. 1056-1061, 2003
22. N. Simond and C. Laurgeau, *Vehicle Trajectory from an Uncalibrated Stereo-Rig with Super-Homography*, IEEE International Conference on Robotics and Systems , pp. 4768-4773, 2006
23. G. Lopez-Nicolas and S. Bhattacharya and J.J. Guerrero and C. Sagues and S. Hutchinson , *Switched Homography-Based Visual Control of Differential Drive Vehicles with Field-of-View Constraints*, IEEE International Conference on Robotics and Automation, 2007
24. J.J Guerrero and R. Martinez-Cantin and C. Sagués , *Visual map-less navigation based on homographies*, Journal of Robotic Systems, pp. 569-581, 2005
25. F. Le Bras and T. Hamel and C. Barat and R. Mahony, *Nonlinear Image-Based Visual Servo controller for automatic landing guidance of a fixed-wing Aircraft*, Proc. of the European Control Conference, pp. 1836-1841, 2009
26. J. R. Azinheira and P. Rives and J. R. H. Carvalho and G. F. Silveira and E. C. de Paiva and S. S. Bueno, *Visual Servo Control for the Hovering of an Outdoor Robotic Airship*, IEEE International Conference on Robotics and Automation, 2002
27. J. R. Azinheira and P. Rives, *Image-Based Visual Servoing for Vanishing Features and Ground Lines Tracking: Application to UAV Automatic Landing*, International Journal of Optomechatronics, vol.2(3), pp. 275-295, 2008